AAEC/E584

AUSTRALIAN ATOMIC ENERGY COMMISSION

RESEARCH ESTABLISHMENT

LUCAS HEIGHTS RESEARCH LABORATORIES

AN X-RAY INVESTIGATION OF AUSTENITE REVERSION IN MARAGING STEELS

by

C.J. BALL

April 1984

ISBN 0 642 59795 2

AUSTRALIAN ATOMIC ENERGY COMMISSION
RESEARCH ESTABLISHMENT
LUCAS HEIGHTS RESEARCH LABORATORIES

AN X-RAY INVESTIGATION OF AUSTENITE REVERSION IN MARAGING STEELS

by

C.J. BALL

ABSTRACT

Reversion of martensite to austenite in maraging steels has been investigated at temperatures in the range 400 to 800°C. Austenite formed at temperatures up to ~680°C does not transform back to martensite on cooling to room temperature, and the amount of such austenite is, in some cases, greater than 65 per cent.

Lattice parameter measurements indicate that substantial amounts of molybdenum and/or titanium remain in solution after completion of the age-hardening precipitation reaction, and that the solubility of these elements is greater in austenite than in martensite at temperatures of ~700°C.

National Library of Australia card number and ISBN 0 642 59795 2

The following descriptors have been selected from the INIS Thesaurus to describe the subject content of this report for information retrieval purposes. For further details please refer to IAEA-INIS-12 (INIS: Manual for Indexing) and IAEA-INIS-13 (INIS: Thesaurus) published in Vienna by the International Atomic Energy Agency.

AUSTENITE; HIGH TEMPERATURE; LATTICE PARAMETERS; MARAGING STEELS; PHASE DIAGRAMS; X-RAY DIFFRACTION

CONTENTS

1. INTRODUCTION 1

2. EXPERIMENTAL 1
   2.1 Materials and Specimen Preparation 1
   2.2 Determination of Amount of Reverted Austenite 1
   2.3 Determination of Lattice Parameters 1

3. RESULTS 2
   3.1 Amount of Reverted Austenite 2
   3.2 Retained Austenite 3
   3.3 Lattice Parameters 3

4. DISCUSSION 3
   4.1 Introduction 3
   4.2 Phase Diagrams 4
   4.3 Amount of Reverted Austenite 4
   4.4 Temperature of Maximum Retention 5
   4.5 Reversion at Low Temperatures 5
   4.6 Lattice Parameters 6

5. CONCLUSIONS 7

6. ACKNOWLEDGEMENT 7

7. REFERENCES 7

Table 1 Compositions of maraging steels (wt%) 9

Table 2 A typical set of intensity measurements, illustrating significance of preferred orientation 9

Table 3 Measured values of $\theta(110)$, with estimated standard deviation from statistical accuracy of peak fitting, for a set of identical specimens 10

Table 4 Variation of lattice parameter of α iron with concentration of solute. 10

Figure 1 Illustration of the accuracy of peak fitting using (a) single Lorentzian function; (b) the sum of two Lorentzian functions representing the $\alpha 1$ and $\alpha 2$ components of the radiation. 11

Figure 2 Determination of the position of a weak 111(γ) peak. 12

Figure 3 Alternative method of determining the position of weak 111(γ) peak. 13

Figure 4 Amount of reverted austenite (γ) retained on cooling to room temperature after a four hour anneal at temperature T - steel A. 14

Figure 5 Amount of reverted austenite (γ) retained on cooling to room temperature after a four hour anneal at temperature T - steel B. 15

(Continued)

Figure 6	Amount of reverted austenite (γ) retained on cooling to room temperature after a four hour anneal at temperature T - steel C.	15
Figure 7	Amount of reverted austenite (γ) retained on cooling to room temperature after a four hour anneal at temperature T - steel D.	15
Figure 8	Amount of reverted austenite (γ) retained on cooling to room temperature after annealing for various times at the temperatures indicated - steel C.	16
Figure 9	Lattice parameters of (a) α phase, and (b) γ phase at room temperature after annealing for four hours at temperature T - steel A.	17
Figure 10	Lattice parameters of (a) α phase, and (b) γ phase at room temperature after annealing for four hours at temperature T - steel B.	18
Figure 11	Lattice parameters of (a) α phase, and (b) γ phase at room temperature after annealing for four hours at temperature T - steel C.	19
Figure 12	Lattice parameters of (a) α phase, and (b) γ phase at room temperature after annealing for four hours at temperature T - steel D.	20
Figure 13	Angular width (full width half maximum, 2θ) of 211α peak after annealing for four hours at temperature T - steel D.	21
Figure 14	Lattice parameters of α (●) and γ (■) phases at room temperature after annealing for various times at the temperatures indicated - Steel C.	22-24
Figure 15	Equilibrium diagram of the Fe-Ni binary system [after Goldstein and Ogilvie 1965].	25
Figure 16	Hypothetical equilibrium diagram of the (Fe,9Co,Mo,Ti)-Ni pseudo-binary system.	26
Figure 17	Equilibrium amounts of austenite at various temperatures, based on the hypothetical pseudo-binary equilibrium diagram of Figure 16.	27

1. INTRODUCTION

Maraging steels are a class of steels that combine high toughness with very high strength. They achieve these properties by the precipitation of intermetallic phases in a matrix of massive martensite. The steels are normally used in the fully martensitic condition but may contain retained or reverted austenite, as a result of faulty heat treatment or introduced deliberately with the intention of increasing toughness at the expense of strength. Peters [1968] has studied reversion at 480°C in a series of alloys. Results are reported of measurements at temperatures in the range 400 to 800°C on three grades of maraging steel, including, for the first time, measurements of lattice parameter.

2. EXPERIMENTAL

2.1 Materials and Specimen Preparation

Two casts of 350 grade steel and one each of 300 and 400 grade were investigated. Results of analyses are given in Table 1. The materials were supplied in the form of extruded and swaged rods of diameter 14 mm. Disc-shaped specimens were cut from the rod and ground to a thickness of approximately 2 mm. These were solution treated for one hour *in vacuo* at 820°C (steels, A,C), 900°C (steel B) or 980°C (steel D), furnace cooled to room temperature and then annealed, again *in vacuo*. No further surface treatment was needed before X-ray examination.

Isothermal measurements were made only on steel C; for these measurements, the same specimen was used for all heat treatments at a given temperature, except for measurements at 500°C. After each anneal, the specimen was cooled to room temperature for X-ray examination and then reheated to the test temperature for the next anneal without an intermediate solution treatment. This procedure is satisfactory for times and temperatures which produce stable structures, but for high temperature anneals, after which the reverted austenite partially transforms back to martensite on cooling to room temperature, a sequence of short anneals is not equivalent to a single anneal for the same total time.

For isochronal measurements, and for isothermal measurements at 500°C, a separate specimen was used for each treatment. Because of the shortage of material, it was necessary, in a few cases, to re-use specimens that had already been heat treated. In these cases, the specimens were solution treated before the second heat treatment.

2.2 Determination of Amount of Reverted Austenite

The amount of reverted austenite was determined by comparison of the integrated intensities of X-ray diffraction peaks of the austenite (γ) and martensite (α) phases [Cullity 1956]. Measurements of integrated intensity were made with a Philips PW1050 goniometer using filtered cobalt radiation. All specimens showed substantial preferred orientation. The extent of the preferred orientation in a typical case is shown in Table 2; for a specimen with no preferred orientation, the values of scaled intensity in column 5 would be the same for all lines of a single phase. The effects of preferred orientation were allowed for, using the B-K method of analysis [Ball and Kelly 1982].

In specimens in which the amount of reverted austenite was less than about 5 per cent, the intensity of the 200(γ) peak, which is used in the B-K method, was too small to be measured accurately. For these specimens, the only austenite line that could be measured accurately was the 111 line, which was measured as described in Section 2.3. In specimens containing more than 5 per cent austenite, where the B-K method was used, the ratio of the scaled intensity of the 111(γ) line to the sum of the scaled intensities of the 111(γ) and 110(α) lines was found to be proportional to the amount of austenite present, indicating that the textures of these specimens were substantially the same. It was assumed that the same relation held in specimens with less than 5 per cent austenite, and it was used to calculate the amount of austenite present in these specimens.

2.3 Determination of Lattice Parameters

Measurements of the angular position of a diffraction line using a diffractometer are subject to a number of systematic errors. The effect of these errors on the derived value of the lattice parameter decreases as the angle of diffraction increases, so the usual procedure is to make measurements on high angle lines only ($2\theta > 90$). However, in many of the samples used in the present work, the amount of austenite present was so small that the only line observable from this phase was the 111 line. Fortunately, changes in lattice parameter are of more interest than absolute values, and these can be

measured quite accurately by careful standardisation of the experimental procedure without eliminating, or correcting for the effects of, systematic errors. All measurements of the lattice parameter of austenite have therefore been made on the 111(γ) line; they may be subject to a systematic error, but the relative values should be reliable.

More lines were observable in the pattern from martensite. However, of the two lines which might have been expected to give the most accurate results, the 310(α) line occurred at too high an angle ($2\theta > 160$), and the 220(α) line was generally so broad and weak that it was difficult to measure. The 200(α) and 211(α) lines were also relatively weak. Measurements of lattice parameter were therefore made on the 110(α) line.

With clearly defined peaks, measurements of peak position were made by step scanning in intervals of 0.02°. The peak position was determined by fitting a parabola or a Lorentzian curve to the data. In later work, allowance was made for the separation of the components of the α doublet by fitting the sum of two Lorentzians, assuming the intensity of $\alpha 2$ to be half that of $\alpha 1$. This did not give a statistically better fit to the data (Figure 1), although it was preferred theoretically. In some cases, the change in lattice parameter was marginally significant, considering only the statistical accuracy of fit. However, since this was not the major source of error, the change was not significant overall, so the earlier data were not re-analysed. It should be noted that the peak profile was not accurately Lorentzian over its full width. Accordingly, the data usually were fitted only down to about half the peak height on either side of the peak.

Reproducibility of the lattice parameter measurement can be gauged from Table 3. All of the specimens listed were heat treated together and so would have had the same lattice parameter. The variation in the observed values of 2θ is greater than can be accounted for by the statistical uncertainty in curve fitting and so must be due to some other source of error.

With a carefully aligned diffractometer, the most serious source of systematic error is displacement of the specimen surface from the diffractometer axis. This source of error was standardised by ensuring that the specimen surface was always, as far as possible, in the same plane. Specimens were pressed into plasticine in a special holder, coincidence of the specimen and holder surfaces being checked by eye, using a straight edge held close to the surfaces. Nevertheless, variation in the position of the specimen surface remains the most likely source of variability in the lattice parameter: a displacement of 10 μm leads to a change in 2θ of 0.005°, which is approximately the magnitude of the random error that was observed. A variation in the position of the specimen surface of ~10 μm seems to be consistent with the specimen mounting technique employed.

For the 211(α) line, the error in lattice parameter resulting from the same variation in the position of the specimen would have been only half as great, but improved accuracy from this source would have been offset by reduced accuracy in locating the peak position, unless much more time had been spent on data collection.

The 111(γ) reflection from specimens with less than about 5 per cent of austenite was very weak and superimposed on a steeply sloping background, of varying slope, arising from the tail of the 110(α) reflection. With these specimens, measurements were made at intervals of 0.05° in 2θ, counting for up to 10^3 seconds at each position. Early data were analysed by first fitting a Lorentzian to the tail of the 110(α) peak, using data points on either side of the 111(γ) peak, then fitting a Lorentzian to the peak produced by subtracting the tail of the 110(α) peak from the original data (Figure 2). This procedure was not entirely satisfactory since it did not fully take into account the tails of the 111(γ) peak. However, neglecting these tails mainly affects the peak area; the 111(γ) peak position is not significantly affected. In later work, the 110(α) tail and 111(γ) peak were fitted in a single analysis (Figure 3). This method of analysis was applied to some of the early data but did not produce a significant shift in peak position, so the rest of the early data was not re-analysed.

3. RESULTS

3.1 Amount of Reverted Austenite

In Figures 4 to 7, the amount of austenite present in a specimen on cooling to room temperature after a 4 h anneal is plotted against the temperature of anneal, for each of the steels investigated. The pattern of behaviour is similar in all cases. For annealing temperatures of 500°C or less, the amount of

austenite is minimal; for higher temperatures, the amount of austenite increases approximately linearly with temperature up to about 680°C, depending on the grade of steel, above which temperature the reverted austenite is unstable on cooling to room temperature and partially transforms back to martensite. In a related investigation, Hemphill [AAEC unpublished data] found, by means of density measurements, that the amount of reverted austenite in these specimens decreases with time at room temperature, the initial rate of change increasing with rises in the annealing temperature. All X-ray measurements were made after several days, or even months, at room temperature, by which time the rate of change of density was negligible.

The amount of austenite present at room temperature in steel C, after annealing for various times at temperatures in the range 500 to 700°C, is shown in Figure 8. At lower temperatures, it appears that no austenite will form, however long the period of anneal. In fact, some austenite present in the sample after a short anneal at 450°C, presumably resulting from an inadequate prior solution treatment, decreased in amount on further annealing and was not detectable after 16 h at 450°C.

The decrease in the amount of austenite present in specimens annealed at 650 or 700°C for the longest times presumably is due to partial transformation back to martensite on cooling to room temperature; for anneals of shorter duration, the austenite formed is stable. The very large difference in the times taken at 650 or 700°C for austenite to become unstable is consistent with the narrowness of the temperature range for the onset of instability after 4 h anneals (Figures 4 to 7).

3.2 Retained Austenite

In specimens of steel D annealed for 4 h at 450 or 500°C, a very weak peak was observed at $2\theta \cong 51°$, corresponding to an interplanar spacing of 0.2078 nm. As the peaks in the two specimens were of approximately the same intensity and appeared at very nearly the same angle, they might have been due to the presence of retained rather than reverted austenite, with a lattice parameter of 0.3600 nm. An identical peak was found in a specimen after solution treatment at 980°C, confirming that the peaks were not due to changes occurring during the 450 or 500°C anneals. They may, however, have been due to the presence of a small amount of μ phase, the strongest line of which has an interplanar spacing of approximately 0.208 nm, depending on composition. According to Warren, Pollock and Kelly [1980], about 0.5 per cent by volume of μ phase of composition $(Fe,Co)_7Mo_6$ would have been present after an anneal for one hour at 980°C, an amount which is certainly of the right order to account for the peaks observed. There is, then, no clear evidence in this work for the presence of retained austenite in steel D after solution treatment at 980°C.

No retained austenite was observed in steels A, B or C after solution treatment at 820 or 900°C.

3.3 Lattice Parameters

The lattice parameters of the austenite and martensite phases in specimens annealed for 4 h at various temperatures are shown in Figures 9 to 12 for all the steels investigated. The sharp increase in lattice parameter of martensite in specimens annealed at temperatures above the maximum temperature for austenite stability is clearly related to the re-formation of martensite. The measured value is the weighted average of the parameters of non-reverted and re-formed martensites. Unfortunately, the resolution, even of the $211(\alpha)$ peak, is not adequate to distinguish the contributions of the two forms. The $211(\alpha)$ peak widths do, however, indicate substantial recovery in internal stress after annealing for 4 h at temperatures in the range 600 to 700°C, with smaller amounts of recovery at lower annealing temperatures (Figure 13).

The variation of lattice parameters with time at temperatures in the range 450 to 700°C is shown for steel C in Figure 14. At each temperature, the lattice parameter of martensite decreases to a value of approximately 0.2869 nm, and the parameter of austenite initially increases to a value of approximately 0.360 nm and then decreases.

4. DISCUSSION

4.1 Introduction

Reversion of martensite to austenite in maraging steels is similar in many respects to austenite reversion in binary Fe-Ni alloys, which can be understood by reference to the equilibrium phase diagram. The relevant part of the Fe-Ni phase diagram is shown in Figure 15 [after Goldstein and

Ogilvie 1965]. In practice, it is found that on cooling a binary Fe-Ni alloy from the γ into the two-phase region, it does not decompose into the equilibrium phases [Allen and Earley 1950]. Instead, on further cooling the austenite transforms, by a shear transformation, to martensite of the same composition. However, on reheating into the two-phase region, the martensite decomposes by a diffusion-controlled reaction to give austenite and ferrite of the equilibrium compositions. This reaction is known as austenite reversion.

Maraging steels are considerably more complex than binary alloys and, in addition to austenite, a number of intermetallic phases may form during a high-temperature anneal. The equilibrium phase diagram is not known, but some insight into the austenite reversion reaction can be obtained by considering a pseudo-binary phase diagram in which nickel is one of the end members. The form of this phase diagram can be guessed at from the binary phase diagrams of iron with each of the major alloying elements, and used to interpret the observed reversion behaviour.

4.2 Phase Diagrams

Addition of small amounts of cobalt to iron has very little effect on the temperature of the γ to α transformation; even 20 per cent of cobalt will increase the temperature by only 40 K [Hansen 1958:471]. Accordingly, it is expected that substitution of cobalt for iron will have little effect on the form of the Fe-Ni phase diagram, and this is confirmed by an isothermal section of the Fe-Ni-Co ternary system [Bradley, Bragg and Sykes 1940]. Molybdenum and titanium, on the other hand, are both strong α-stabilisers, their binary phase diagrams with iron containing closed γ-loops with vertices at about 3 and 1 wt%, respectively, of alloying addition [Hansen 1958:668,723]. Hence more nickel will be required to stabilise the γ-phase in maraging steels than in Fe-Ni alloys, *i.e.* the γ phase boundary will be shifted to higher nickel contents and temperatures.

There is one very important difference between the true Fe-Ni binary system and the pseudo-binary system considered here. In the Fe-Ni system, the composition of the product γ phase is given by the γ phase boundary, and during an isothermal reaction it does not change. However, in maraging steels the effective position of the boundary depends on the amounts of molybdenum and titanium in solution, and so will be affected by formation of intermetallic phases and by diffusion in the vicinity of phase interfaces, which may occur during the reversion reaction.

4.3 Amount of Reverted Austenite

The equilibrium amount of reverted austenite at any temperature is determined by partitioning the available nickel between the α and γ phases, with compositions given by the phase boundaries at that temperature. However, on cooling to room temperature, austenite will transform to martensite, at least partially, if its nickel content is less than a certain amount which, according to Peters [1968], is about 30 per cent for binary Fe-Ni alloys. The greatest amount of austenite will therefore be observed in specimens that have been annealed at the temperature for which the γ-phase boundary has this critical composition, and the amount observed will be determined by the amount of nickel available.

The maximum amount of austenite observed (65 per cent in steels A, B and C) is of the right order of magnitude but somewhat higher than expected from the above argument. If we assume a nickel content of 4 per cent at the α phase boundary and an overall ($\alpha + \gamma$) nickel content of 18 per cent in these steels, then the nickel content of 65 per cent of austenite would be only 25.5 per cent. This is slightly less than the figure of 27 per cent quoted by Jones and Pumphrey [1949]. In steel D, the maximum amount of austenite observed is only 50 per cent, but the nickel content of this steel is ~13 per cent so, with the same assumptions as before, the nickel content of the austenite is only 22 per cent.

There are two possible explanations for the large amount of austenite observed. First, it is possible that the nickel content of the austenite is as given above and that this is sufficient to give it stability at room temperature in maraging steels. Yeo [1963] investigated the effects of some alloying elements on the martensitic transformation temperature of Fe-22.5Ni base alloys. He found that cobalt and small amounts of titanium raised the transformation temperature whereas it was lowered by molybdenum. Simple addition of the (extrapolated) effects of 9 per cent of cobalt and 5 per cent of molybdenum would suggest that the transformation temperatures of maraging steels would be greater than those of Fe-18Ni alloys, *i.e.* that more nickel would be required to stabilise austenite at room temperature, but Yeo also noted that the effect of an alloying element depends on the properties of the base alloy to which the addition is made. This implies that the effects of two or more alloying additions are not

necessarily additive.

The second possibility is that the average composition of the ($\alpha + \gamma$) phases differs from the overall composition of the steel owing to the precipitation of one or more intermetallic phases. The most commonly reported precipitates in maraging steels are Fe_2Mo, Ni_3Mo and Ni_3Ti. Of these, precipitation of Ni_3Mo or Ni_3Ti would reduce the average nickel content of the ($\alpha + \gamma$) phases and so make the stability of large amounts of austenite harder to explain; but, in any of the steels, precipitation of about half the molybdenum as Fe_2Mo would increase the average nickel content of the remainder sufficiently to form the observed amount of austenite with a nickel content of about 27 per cent. It should be noted that this argument for formation of Fe_2Mo applies only to the precipitates formed at temperatures near 650°C, and the precipitate formed during a normal hardening anneal at 485°C may well be different.

4.4 Temperature of Maximum Retention

Figures 4 to 7 imply that, for each steel, there is a well-defined temperature for maximum retention of austenite on cooling to room temperature, as is the case for binary Fe-Ni alloys, but Figure 8 shows that such is not the case and that the temperature of maximum retention is related to the time of anneal. For steel C, the annealing temperature which gives maximum retention after a four hour anneal is approximately 680°C, yet austenite formed in this steel after 100 h at 650°C is unstable, and after 10 min at 700° is stable. These results presumably are related to time-dependent concentrations of molybdenum and titanium in the austenite, caused by precipitation of intermetallic phases and diffusion between austenite and ferrite, which cause the nickel content of the austenite also to vary. However, the salient point is not that the nickel content of austenite is time-dependent but that it is very much larger in maraging steels than it would be in an Fe-Ni alloy at the same temperature.

It is tempting to try to assess the relative efficacy of molybdenum and titanium in shifting the γ phase boundary to higher nickel contents and temperatures, but the data obtained in this investigation do not allow any conclusions to be reached. The reason for this is that an unknown amount of the alloying additions in each steel is in the form of precipitates. Note that the temperature of maximum austenite retention in steel D (~690°C) is nearly the same as in the other steels, despite a much higher total molybdenum content.

4.5 Reversion at Low Temperatures

The most significant difference between the steels in the lower range of temperatures is the greater amount of reversion that takes place in steel A. This must be attributed to the smaller amount of titanium in this steel than in steels B and C. Peters [1968] observed a similar effect with titanium in Fe-17Ni base alloys aged at 480°C for much longer times; he attributed this to the formation of Ni_3Ti. Supposedly, 1.4 wt% of titanium absorbs about 5.0 wt% of nickel and the matrix then behaves as though it were a 12 per cent Ni alloy. This interpretation is consistent with the observations, but the only firm conclusion that can be drawn is that the matrix composition is relatively closer to the α phase boundary in the titanium-bearing steel, which could be due to a shift in the phase boundaries rather than to a shift in matrix composition. As noted earlier, in connection with the stability of austenite formed at high temperatures, the γ phase boundary is shifted to a higher nickel content in steels containing molybdenum and titanium, and it is reasonable to expect that the α phase boundary would be similarly affected, with both shifts decreasing the equilibrium amount of austenite at a given temperature.

The relevant pseudo-binary phase diagram is not known, but if the α and γ phase boundaries can be approximated by straight lines, then an indication of the locations of these lines can be obtained from the estimated temperature of complete reversion (750°C), the temperature of maximum austenite retention on cooling to room temperature (675°C, assumed to correspond to a nickel content of ~27 per cent), and the equilibrium amounts of austenite at high temperatures. From a phase diagram constructed in this way (Figure 16), the equilibrium amount of austenite at any temperature can be calculated (Figure 17). The calculation is subject to considerable uncertainty but, nevertheless, it shows quite clearly not only that the amounts of austenite observed after four hours at the lower temperatures are not the equilibrium amounts, which is already apparent from Figure 8, but that the equilibrium amounts cannot be predicted reliably from Figure 8. Presumably, the amount of austenite formed in four hours is more indicative of the ease of nucleation or rate of diffusion than of the equilibrium amount. It is not clear why titanium should have any effect, which merely underlines the fact that nothing is known about the nucleation process.

A surprising feature of the reversion behaviour in steels A, B and C is the presence of small amounts (~1 per cent) of austenite after four hour anneals at 400 or 450°C. Apart from the specimen of steel C annealed at 450°C, which was solution treated in the 'as received' condition, all the specimens had been annealed at temperatures in the range 650 to 700°C before the final solution treatment. As noted earlier, no austenite could be detected after solution treatment, but it is quite likely that this anneal is not adequate to eliminate completely the variations in composition caused by the earlier anneals. To what extent such small amounts of austenite affect the mechanical properties is not known.

4.6 Lattice Parameters

The lattice parameter of an alloy depends on the amounts of the various alloying additions that are in solution, and so can be used to monitor changes in these amounts. Of the major alloying additions in maraging steels, cobalt has practically no effect on the lattice parameter of the α phase, nickel increases it slightly and molybdenum and titanium both increase it substantially (Table 4). According to King [1966], lattice parameter changes for solutions of the same solute in different structural forms of a solvent agree quite closely, so the same is expected to be true of the γ phase.

The isothermal data from steel C (Figure 14) show a rapid initial decrease in the lattice parameter of the α phase, with no apparent incubation period. Most of the change occurs before significant amounts of austenite are formed, and clearly is due to precipitation of intermetallic phases containing molybdenum and titanium. The magnitude of the change is approximately 0.0006 nm, which corresponds to a change of about 3.4 wt% in the amount of molybdenum or 1.7 wt% of titanium in solution.

During subsequent annealing there is a continuing small reduction in the α parameter, while austenite is being formed, the additional change being ~0.0001 nm at 600°C (Figure 14). This is less than would be expected from the probable change in nickel content of the α phase (~15 per cent), but the accuracy of the measurement is not adequate to say whether this is the only change that is taking place. Even with more accurate measurements, the question could still not be answered with certainty, since the variation of lattice parameter with nickel content has not been established for the relevant range of concentrations. The most recent work in this field [Sutton and Hume-Rothery 1955] suggests that the value given in Table 4 overestimates the effect of nickel at high concentrations. If this is the case, it could indicate a continuing decrease in the molybdenum and/or titanium contents of the α phase.

For annealing treatments which cause the reverted austenite to be unstable on cooling to room temperature, the measured value of the α parameter is the mean of the parameters of the high temperature α phase and re-formed martensite. Unfortunately, the resolution is not adequate to distinguish the two phases, but for temperatures close to the critical temperature for austenite stability, the amounts of the two phases and the parameter of the high-temperature α phase can be estimated by extrapolation of data at subcritical temperatures, hence the parameter of the re-formed martensite can also be estimated. Values obtained in this way are substantially greater than those for the high-temperature α phase, but less than the values for solution treated material. This indicates that the concentrations of molybdenum and/or titanium in solution in austenite at these temperatures are greater than the concentrations in the α phase, since the difference in parameter cannot be explained solely by the greater nickel content of the austenite.

The changes in the α parameter are consistent with the idea that the precipitate formed in the α phase subsequently dissolves in austenite. This probably happens, but that it is not the whole story is shown by the variation of the γ parameter. The pattern of behaviour of γ parameters is seen most clearly in the isothermal measurements on steel C at 600°C (Figure 14). The parameter is low initially, rises to a maximum after about four hours and then slowly falls. The rates of both rise and fall increase with increase of temperature, so the parameter observed after a four hour anneal at other temperatures will be before the peak for temperatures below about 600°C and beyond it for higher temperatures. The isochronal data of Figures 9 to 12 therefore show a broad peak centred at about 600°C.

The initial rise can be attributed to the dissolution of a precipitate that contains molybdenum and/or titanium, but the subsequent fall suggests that either Mo/Ti is diffusing into the α phase or another precipitate is forming in the austenite. Diffusion of Mo/Ti into the α phase would not necessarily increase the α parameter, since it would probably lead to growth of the existing precipitates

with no increase in the amounts of molybdenum or titanium in solution. Since a reduction of the Mo/Ti content of austenite would result in the pseudo-binary phase boundary shifting to a lower nickel concentration, diffusion of molybdenum and/or titanium would be expected to be accompanied by diffusion of nickel, or by growth of the austenite, leading in either case to a reduction in the concentration of nickel and so to reduced stability of the austenite, as observed. However, the observations could be explained equally well by precipitation of a (Ni,Mo,Ti) intermetallic phase. The data presented here are not adequate to distinguish between these two possibilities.

5. CONCLUSIONS

The conclusions of this investigation are, for the most part, embodied in the data presented in Figures 4 to 14. However, the following points merit special emphasis.

(a) The amount of reverted austenite that remains stable on cooling to room temperature can be very large in relation to the amount of nickel in the steel. In some instances, the concentration of nickel in this austenite is not more than about 25 per cent.

(b) Microsegregation caused by the partial formation of austenite is not eliminated by the standard solution treatment of one hour at 820, 900 or 980°C, and can lead to formation of austenite during annealing at the age-hardening temperature.

(c) Austenite formed at temperatures of 650°C and above can be stable at room temperature.

(d) The stability of austenite decreases with time at temperatures in the range 650 to 700°C.

(e) Loss of stability is associated with reduction in the amounts of molybdenum and/or titanium in solution in austenite. This could be due to diffusion, or to precipitation of an intermetallic phase.

6. ACKNOWLEDGEMENT

Thanks are due to R.J. Hemphill for fabrication and heat treatment of most of the specimens used in this investigation.

7. REFERENCES

Allen, N.P. and Earley, C.C. [1950] - *J. Iron Steel Inst.,* 166: 281.

Ball, C.J. and Kelly, P.M. [1982] - *Met. Sci.,* 16: 332.

Bradley, A.J., Bragg, W.L. and Sykes, C. [1940] - *J. Iron Steel Inst.,* 141: 63.

Cullity, B.D. [1956] - Elements of X-Ray Diffraction. Addison-Wesley, Reading, Mass., p:391.

Goldstein, J.I. and Ogilvie, R.E. [1965] - Goddard Space Flight Center Report NASA TM-X-55248.

Guljaev, A.P. and Trusova, E.F. [1950] - *Zh. Tekh. Fiz.,* 20:66.

Hansen, M. [1958] - Constitution of Binary Alloys. McGraw-Hill, New York.

Jones, F.W. and Pumphrey, W.I. [1949] - *J. Iron Steel Inst.,* 163: 132.

King, H.W. [1966] - *J. Mater. Sci.,* 1:79.

Peters, D.T. [1968] - *ASM Trans. Q.* 61: 62.

Sutton, A.L. and Hume-Rothery, W. [1955] - *Phil. Mag.,* 46:1295.

Warren, R.B., Pollock, J.T.A. and Kelly, P.M. [1980] - AAEC/E483.

Yeo, R.B.G. [1963] - *Trans. Metall. Soc. AIME,* 227: 884.

Zwell, L. and Wriedt, H.A. [1972] - *Metall. Trans.,* 3:593.

TABLE 1
COMPOSITIONS OF MARAGING STEELS (wt%)

Element	A	B	C	D
Ni	17.8	18.15	18.15	13.2
Co	7.8	10.8	na	13.1
Mo	4.9	4.4	4.4	9.5
Ti	0.5	1.46	1.30	0.1
Al	0.16	0.17	0.11	0.005
V	0.01	<0.01	na	0.01
Cr	0.01	<0.01	na	<0.01
Mn	0.04	0.03	na	0.01
Cu	0.02	0.01	na	0.01
Nb	<0.01	<0.01	na	<0.01
B	0.004	0.004	na	0.002
C	0.0075	0.002	0.005	0.002
N	0.001	0.002	<0.001	0.0025
Si	0.05	0.04	0.02	0.04
P	0.002	0.004	0.003	0.003
S	0.004	0.007	0.005	0.006
Fe	balance	balance	balance	balance

na not analysed

TABLE 2
A TYPICAL SET OF INTENSITY MEASUREMENTS, ILLUSTRATING SIGNIFICANCE OF PREFERRED ORIENTATION

Phase	hkl	I	I_o	I/I_o
	110	464	22.76	20.39
	200	19	3.02	6.29
	211	72	6.19	11.63
	220	50	2.84	17.61
	111	537	16.47	32.60
	200	146	7.27	20.08
	220	38	3.86	9.84
	311	98	5.53	17.72
	222	54	1.84	29.35

a. Observed integrated intensity is in arbitrary units.

b. I_o = p L f exp(-2M), where p is the multiplicity factor, L is the Lorentz polarisation factor, f is the atomic scattering factor, and exp(-2M) is the temperature factor

TABLE 3
MEASURED VALUES OF 2θ (110), WITH ESTIMATED STANDARD DEVIATION FROM STATISTICAL ACCURACY OF PEAK FITTING, FOR A SET OF IDENTICAL SPECIMENS

Specimen	2θ (110)	a(nm)
84	52.2296(9)	0.28758
85	52.2223(12)	0.28762
86	52.2170(8)	0.28765
87	52.2209(7)	0.28763
88	52.2217(20)	0.28762
89	52.2312(7)	0.28758

$2\theta = 52.2238(55)$

a $= 0.28761(2)$ nm

TABLE 4
VARIATION OF LATTICE PARAMETER OF α IRON WITH CONCENTRATION OF SOLUTE

Element	f*	Reference
Co	0.000077	Sutton and Hume-Rothery [1955]
Ni	0.000053	
Mo	0.000175	Guljaev and Trusova [1950]
Ti	0.000363	Zwell and Wriedt [1972]

* $\Delta a = f \times$ (wt% solute) nm

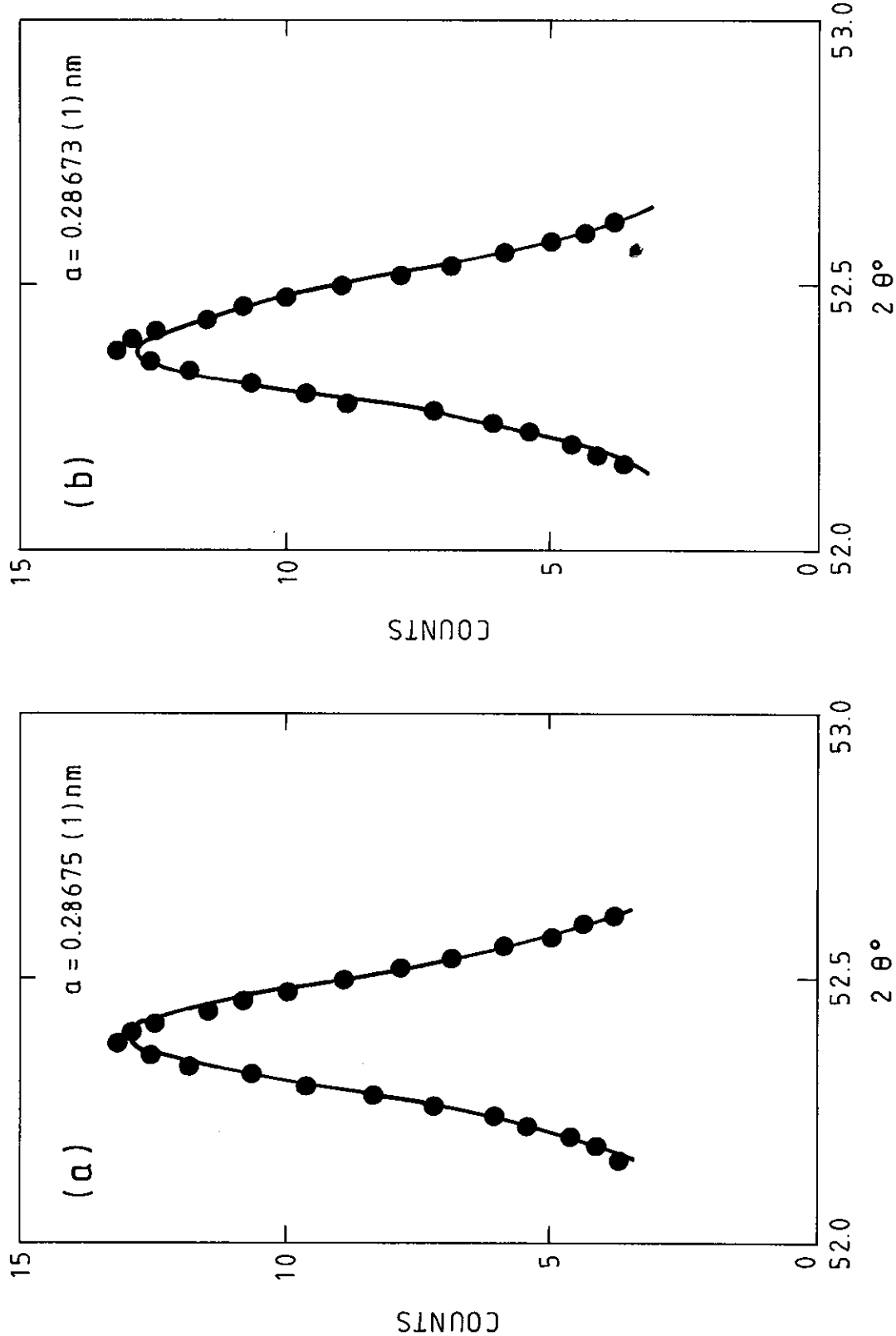

FIGURE 1 Illustration of the accuracy of peak fitting using (a) single Lorentzian function; (b) the sum of two Lorentzian functions representing the $\alpha 1$ and $\alpha 2$ components of the radiation. The same set of data points is fitted in both cases.

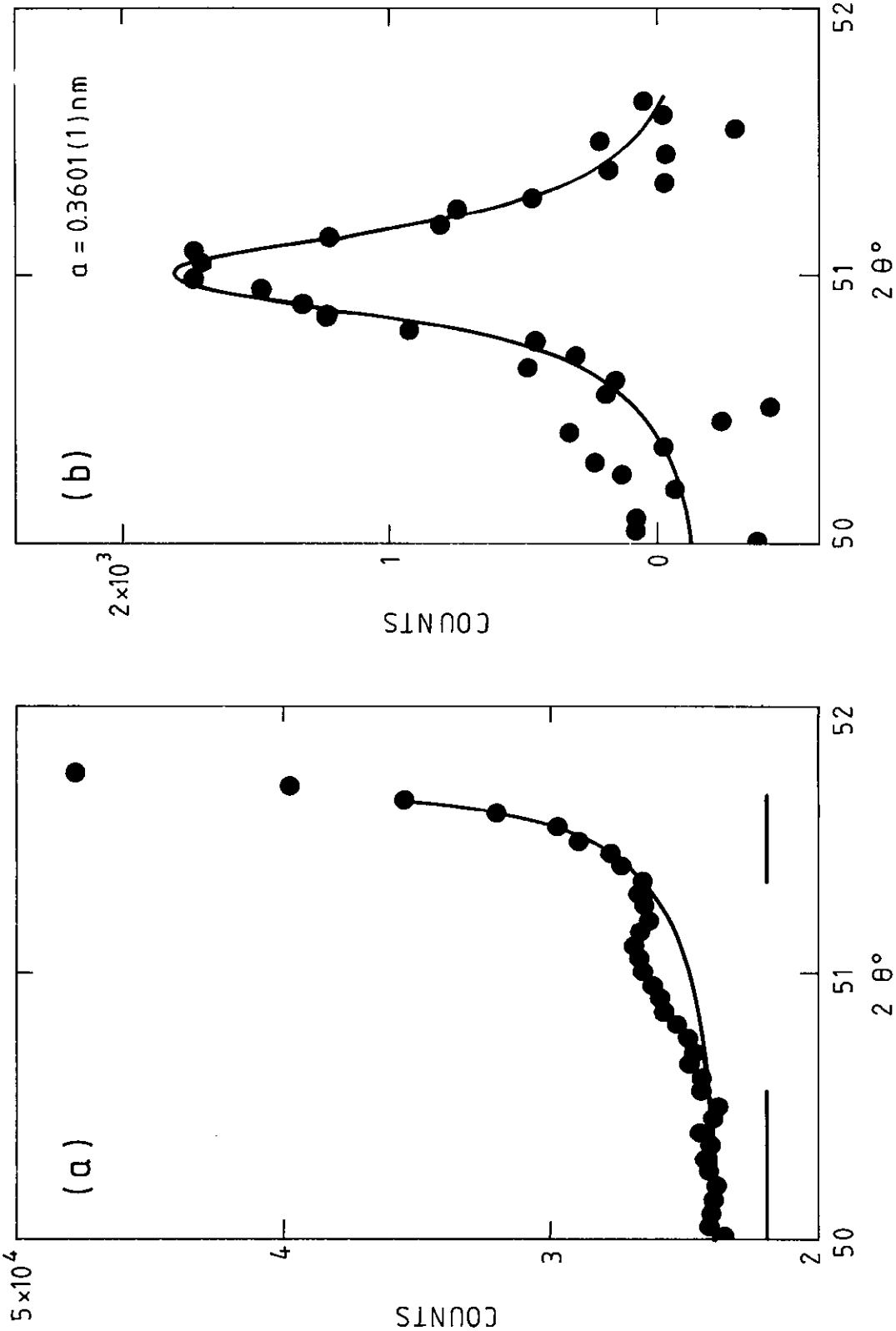

FIGURE 2 Determination of the position of a weak 111(γ) peak. (a) Original data points with background fitted over angular ranges indicated by bars. (b) Lorentzian function fitted to data obtained by subtracting background from original data.

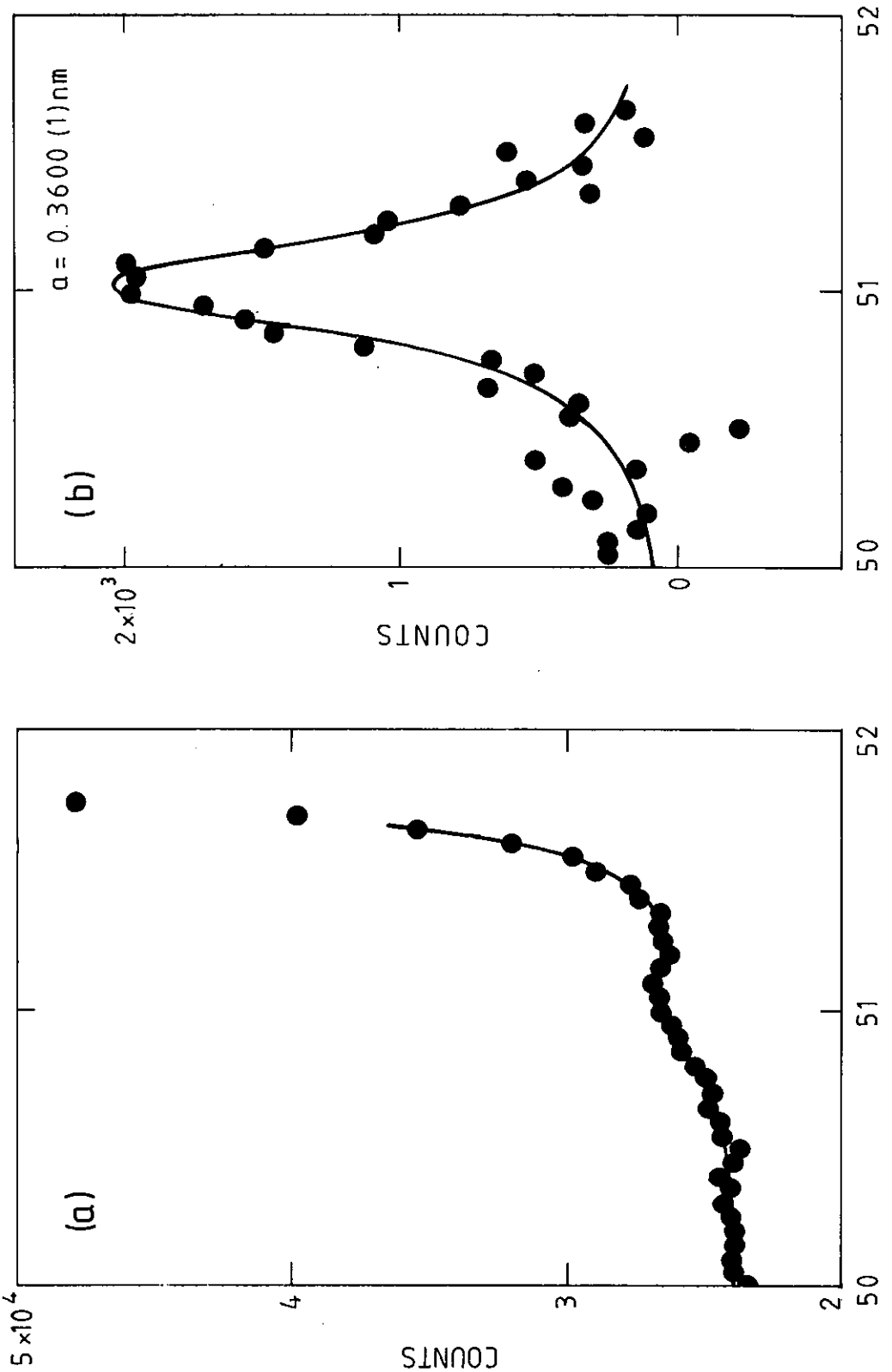

FIGURE 3 Alternative method of determining the position of weak 111(γ) peak. (a) Data of Figure 2 fitted simultaneously by Lorentzian function and background function, assumed to be a Lorentzian function centred on position of 110(γ) peak. (b) Data obtained by subtracting background from original data, with Lorentzian function fitted in (a).

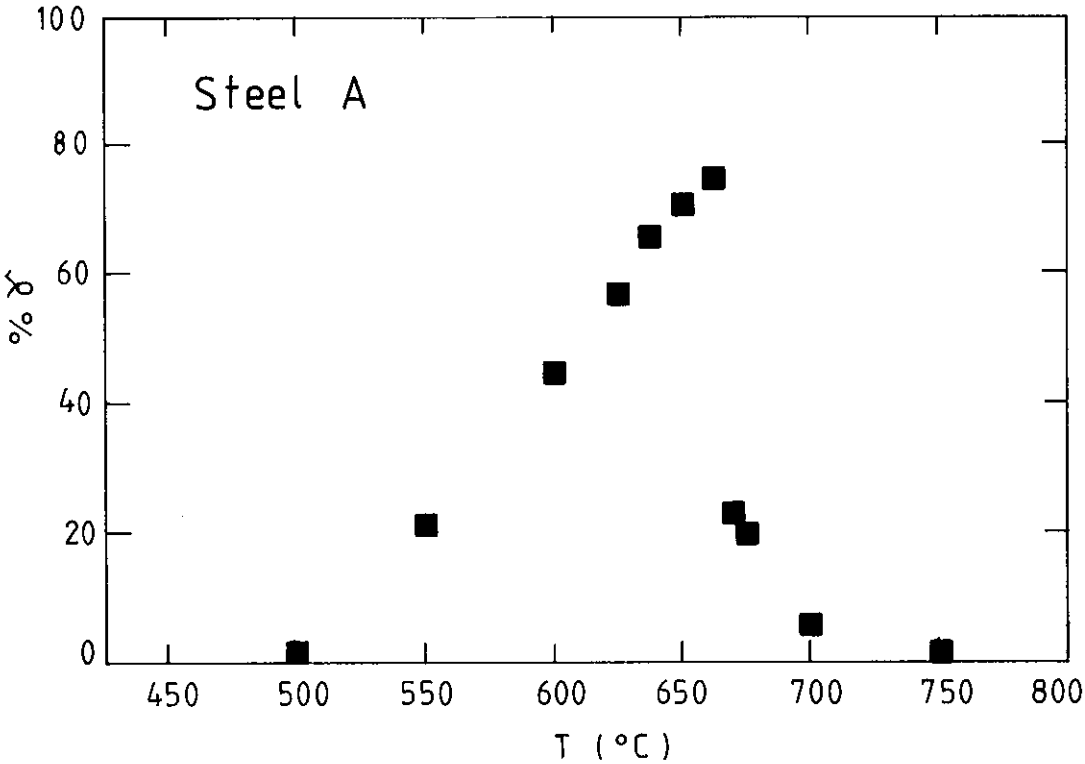

FIGURE 4 Amount of reverted austenite (γ) retained on cooling to room temperature after a four hour anneal at temperature T - steel A.

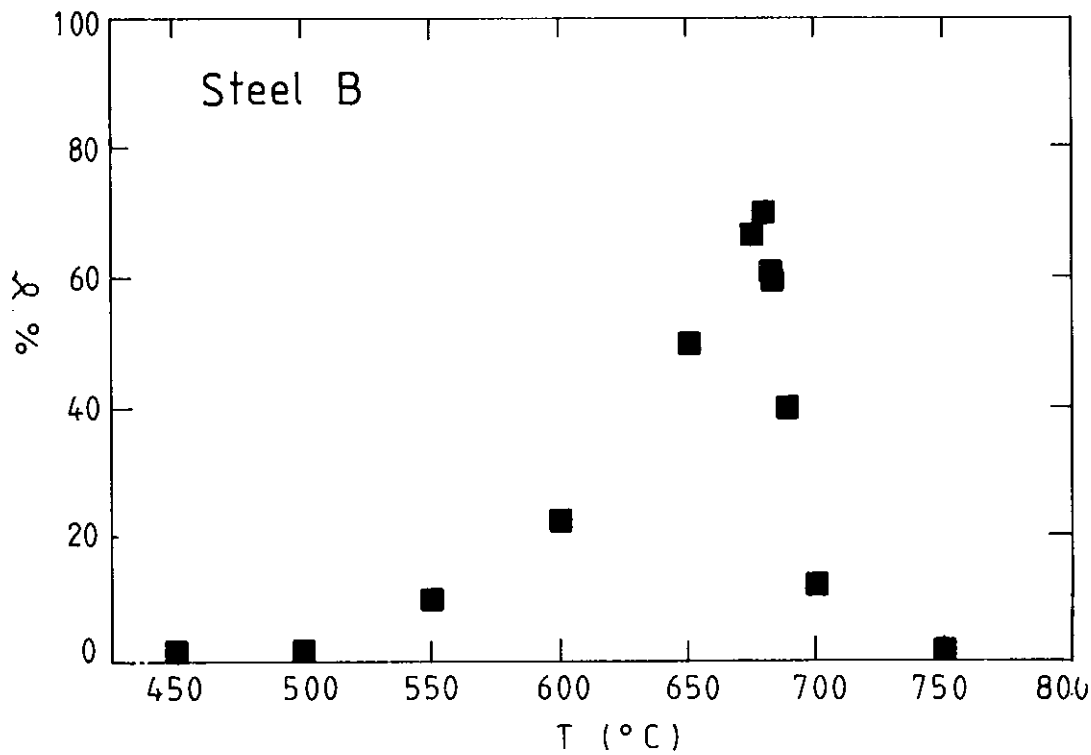

FIGURE 5 Amount of reverted austenite (γ) retained on cooling to room temperature after a four hour anneal at temperature T - steel B.

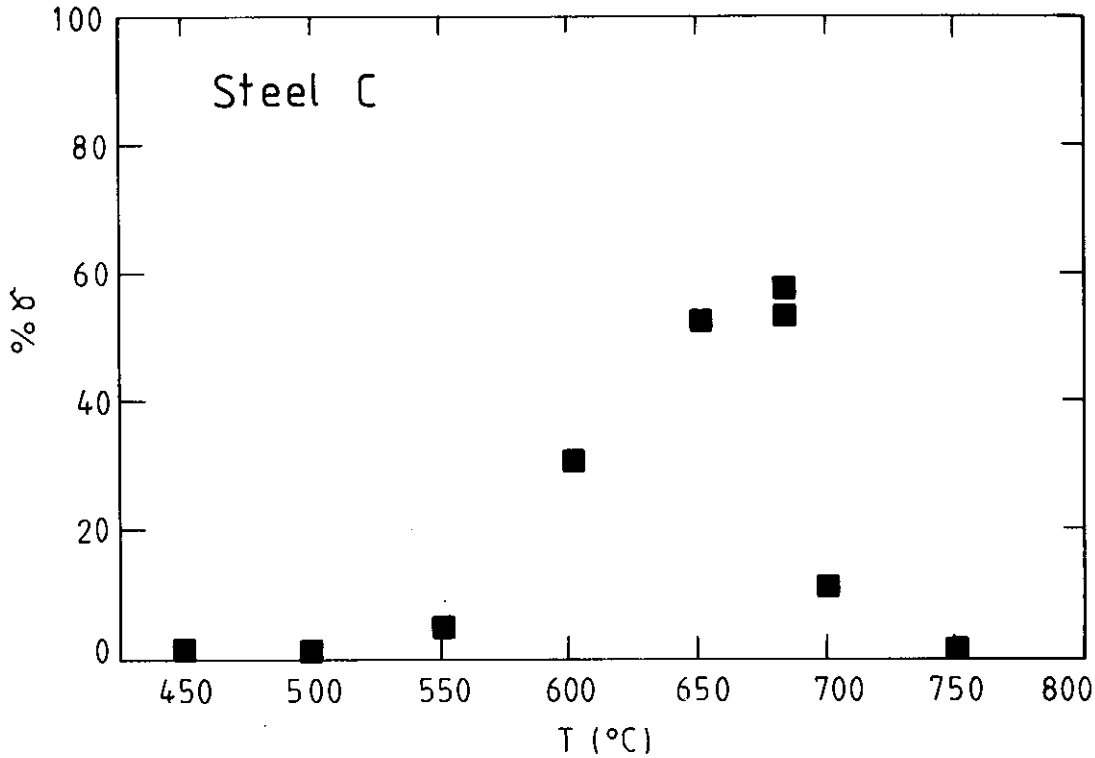

FIGURE 6 Amount of reverted austenite (γ) retained on cooling to room temperature after a four hour anneal at temperature T - steel C.

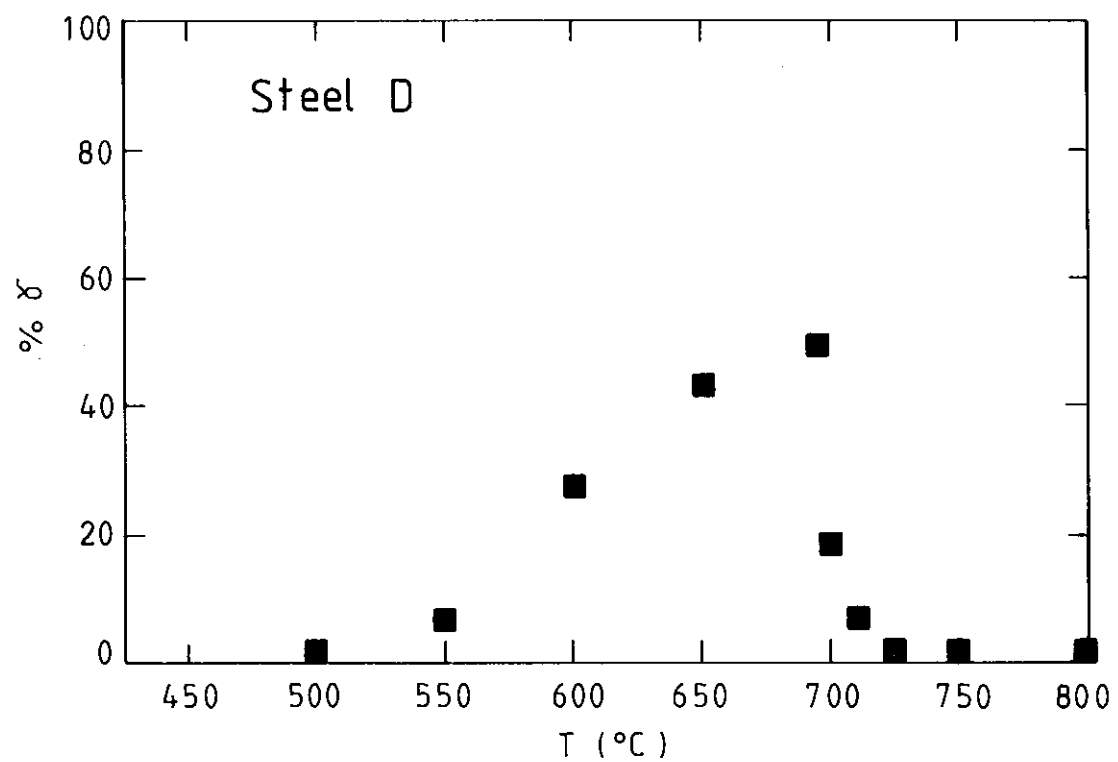

FIGURE 7 Amount of reverted austenite (γ) retained on cooling to room temperature after a four hour anneal at temperature T - steel D.

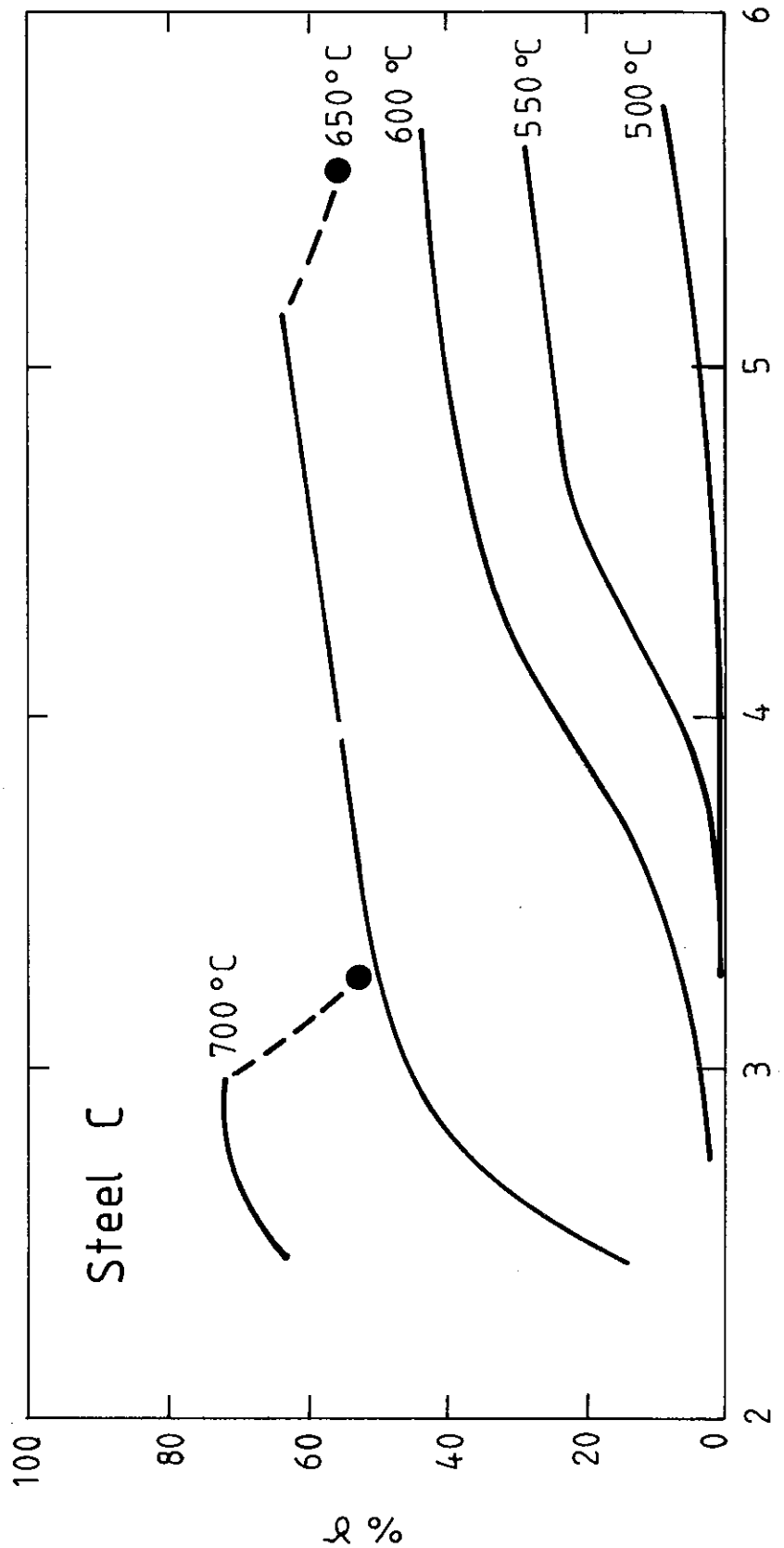

FIGURE 8 Amount of reverted austenite (γ) retained on cooling to room temperature after annealing for various times at the temperatures indicated - steel C.

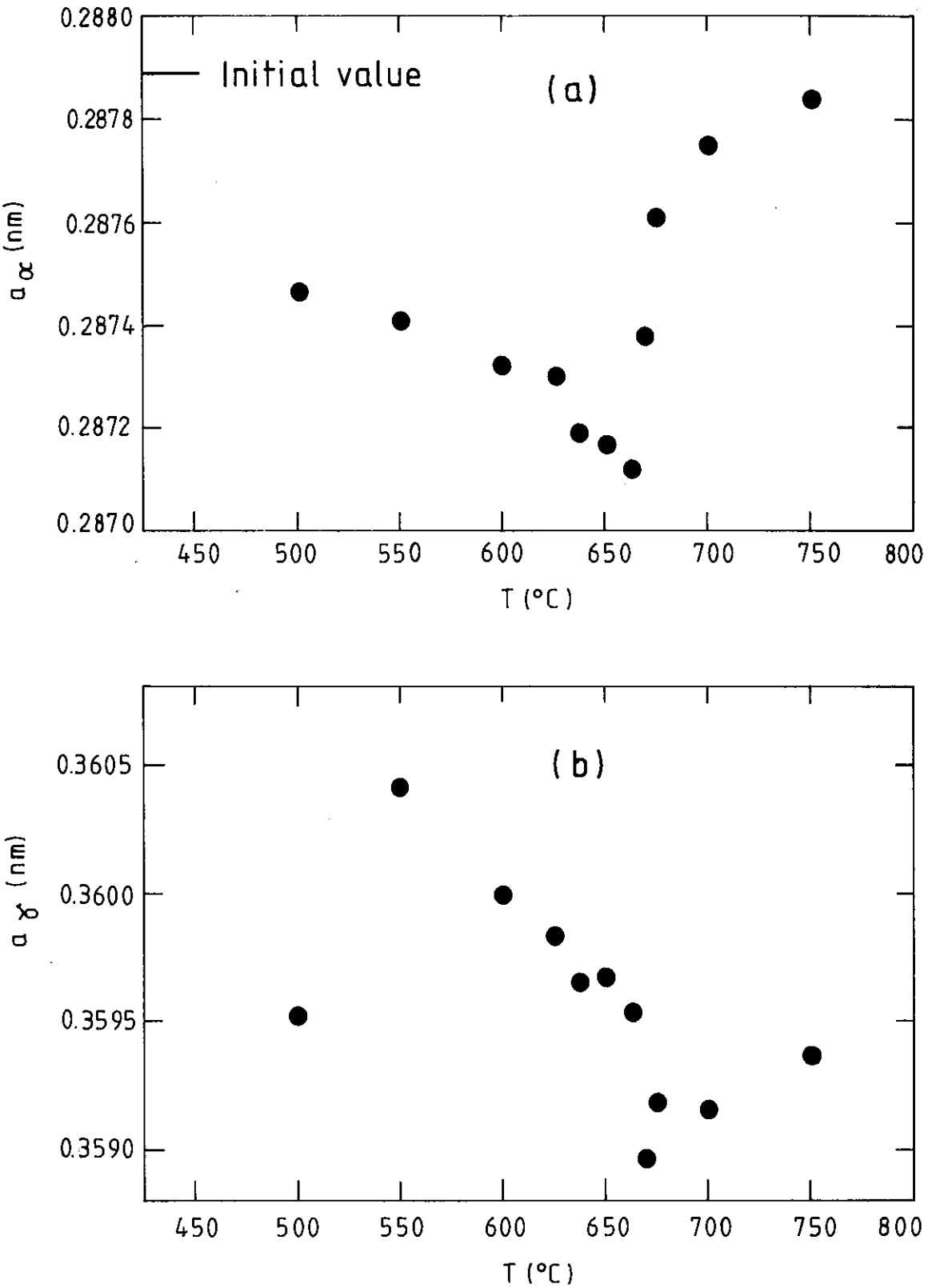

FIGURE 9 Lattice parameters of (a) α phase, and (b) γ phase at room temperature after annealing for four hours at temperature T - steel A.

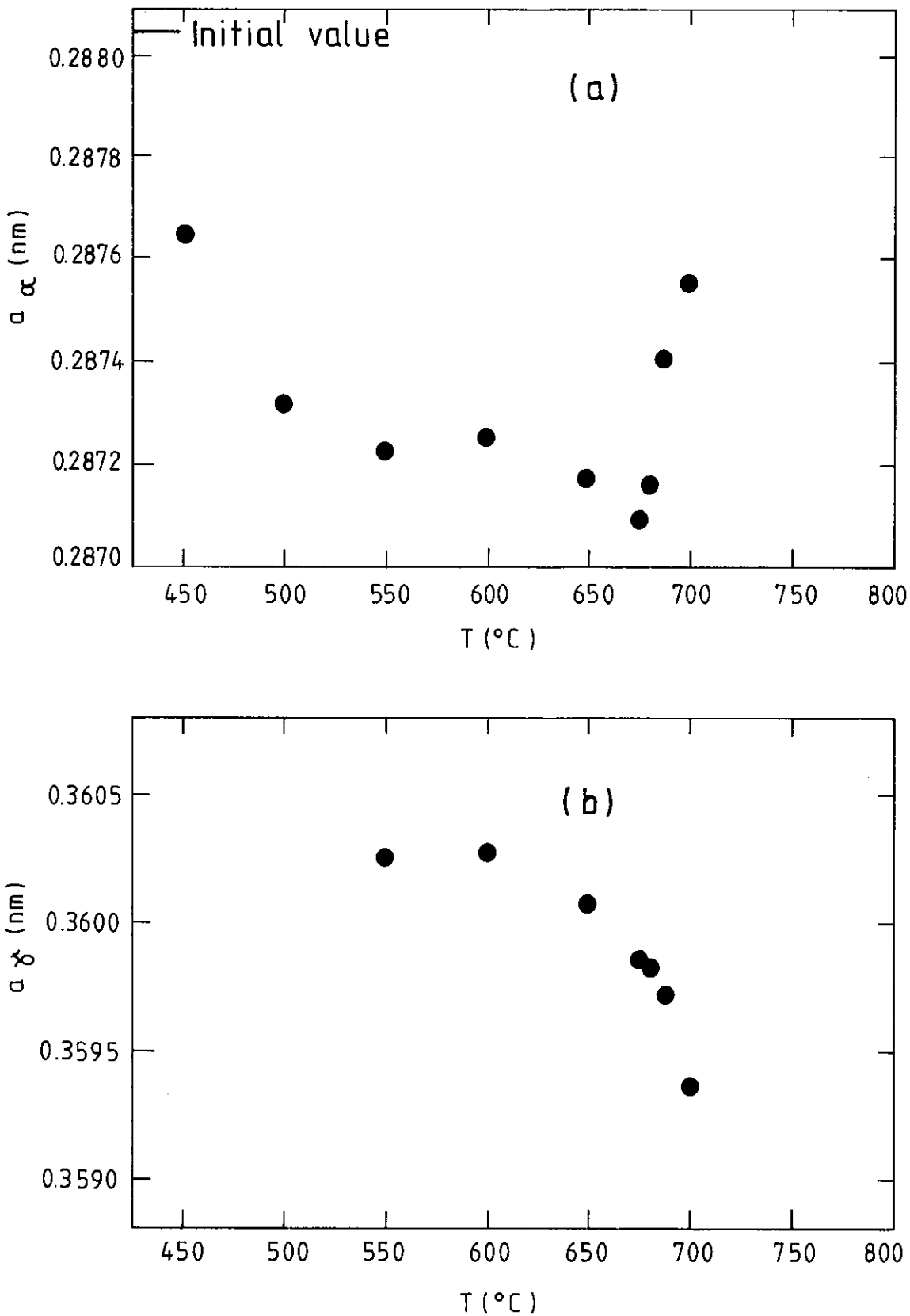

FIGURE 10 Lattice parameters of (a) α phase, and (b) γ phase at room temperature after annealing for four hours at temperature T - steel B.

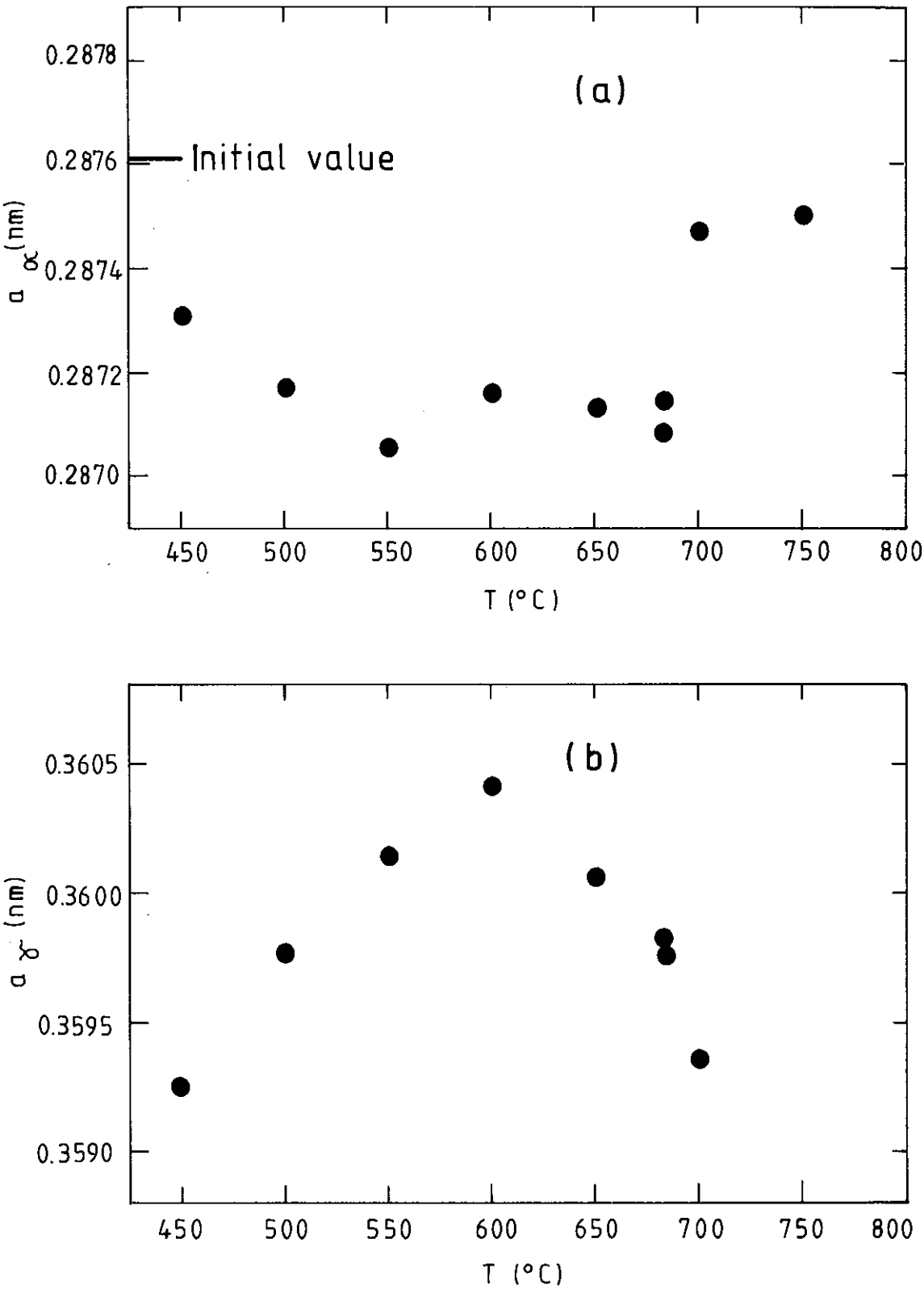

FIGURE 11 Lattice parameters of (a) α phase, and (b) γ phase at room temperature after annealing for four hours at temperature T - steel C.

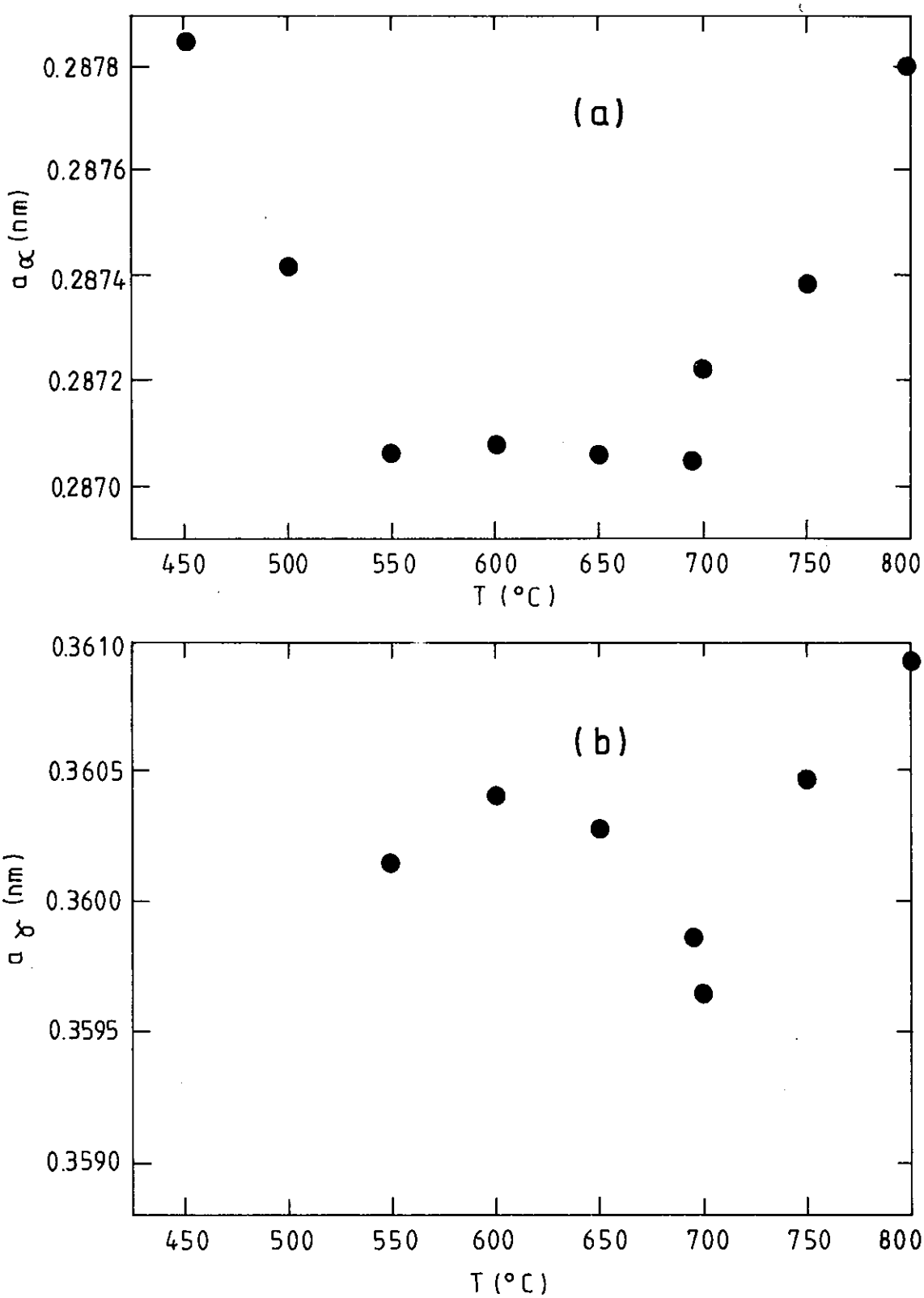

FIGURE 12 Lattice parameters of (a) α phase, and (b) γ phase at room temperature after annealing for four hours at temperature T - steel D.

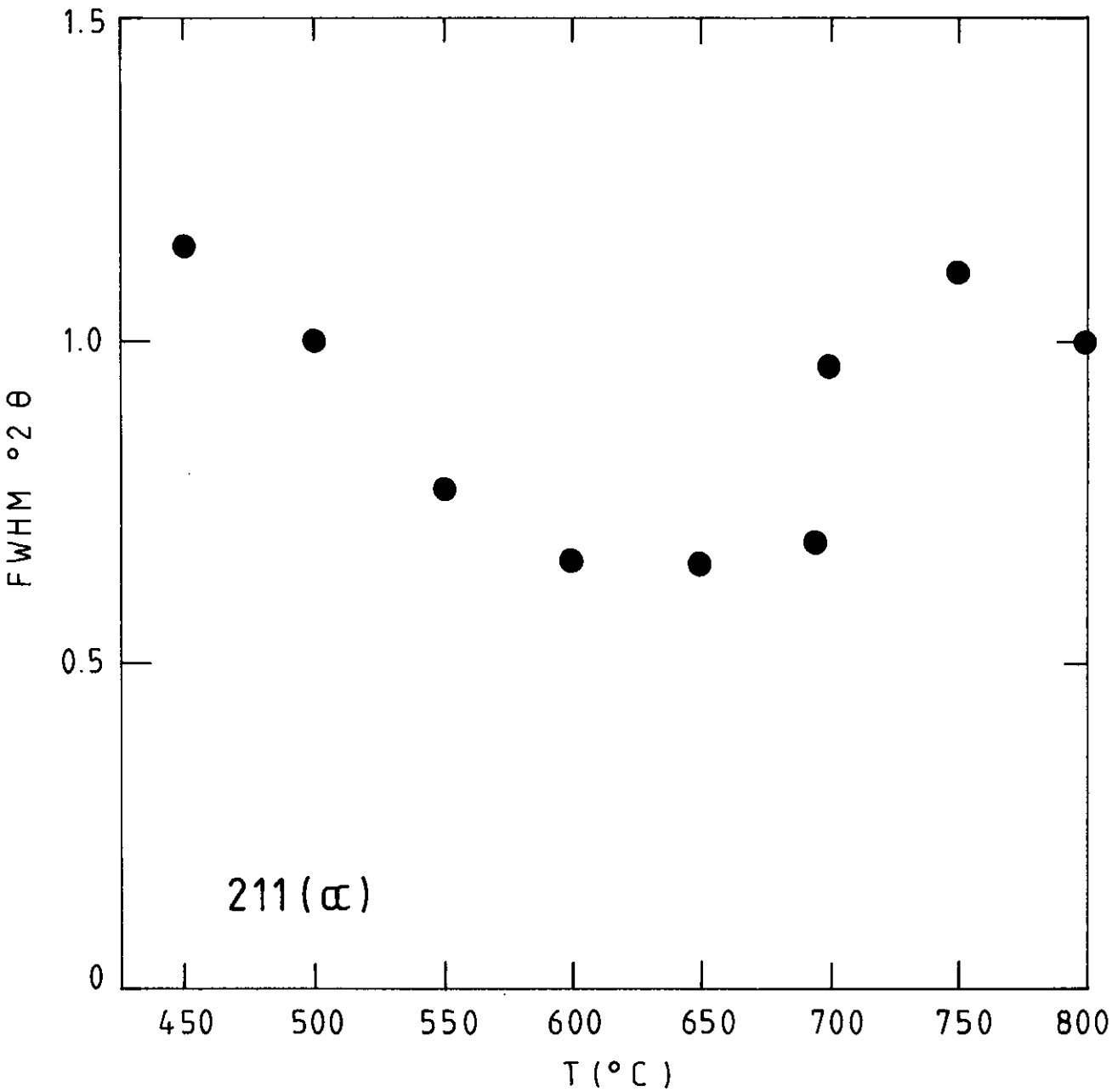

FIGURE 13 Angular width (full width half maximum, 2θ) of 211α peak after annealing for four hours at temperature T - steel D.

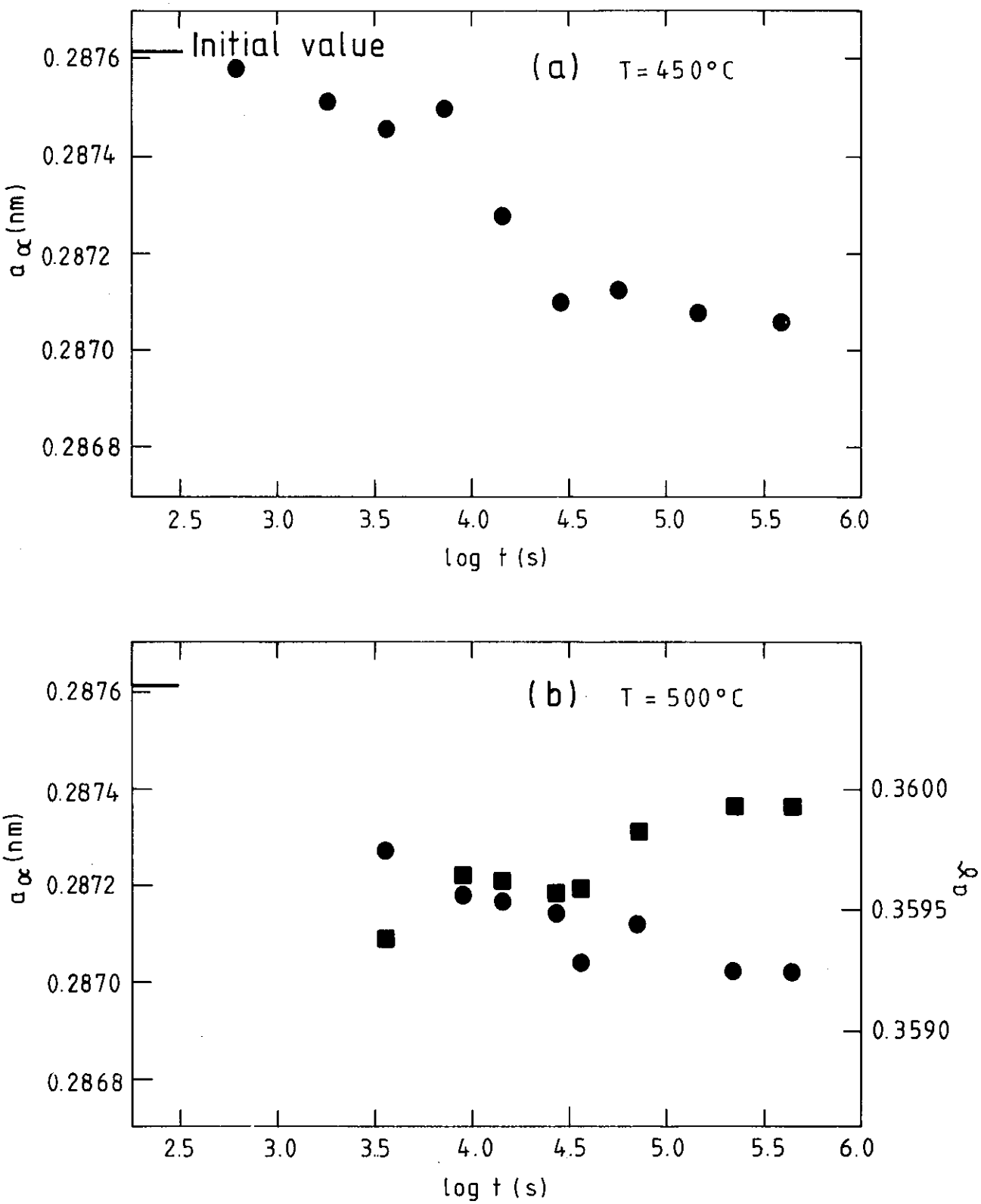

FIGURE 14a-e Lattice parameters of α (●) and γ (■) phases at room temperature after annealing for various times at the temperatures indicated - Steel C.

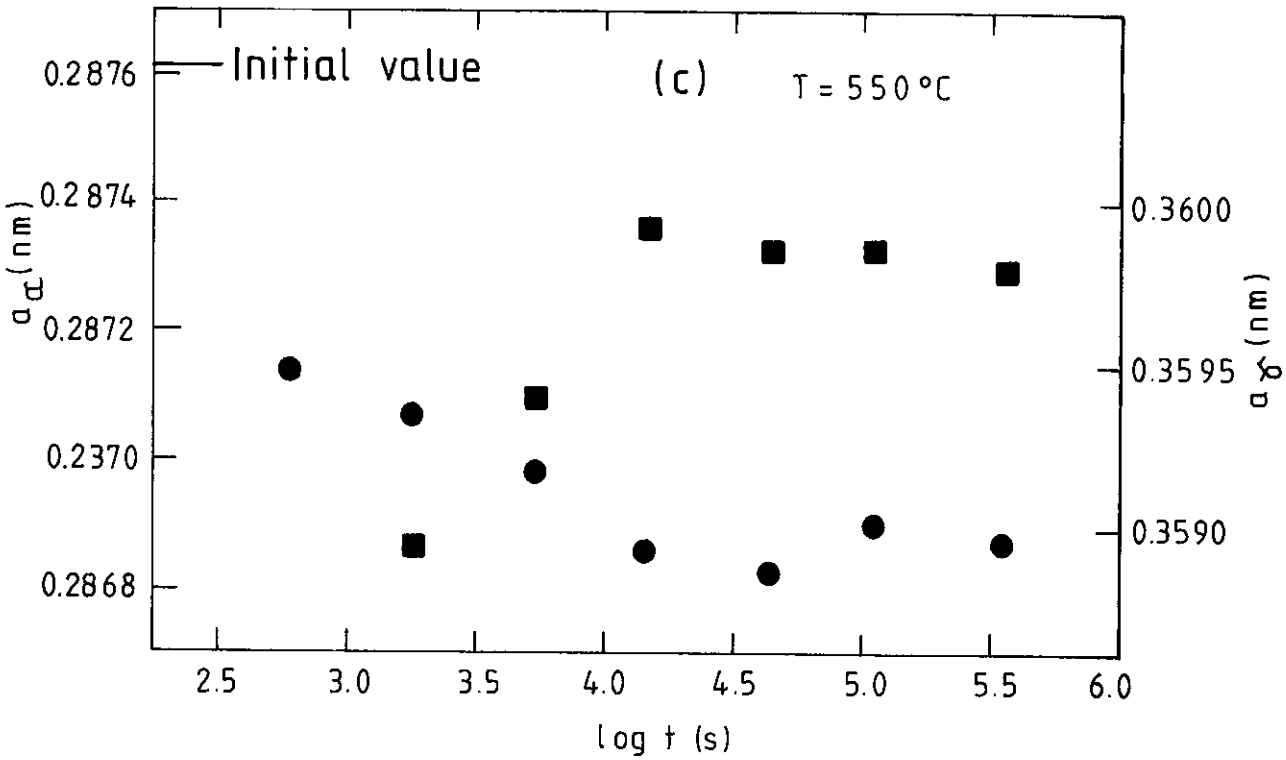

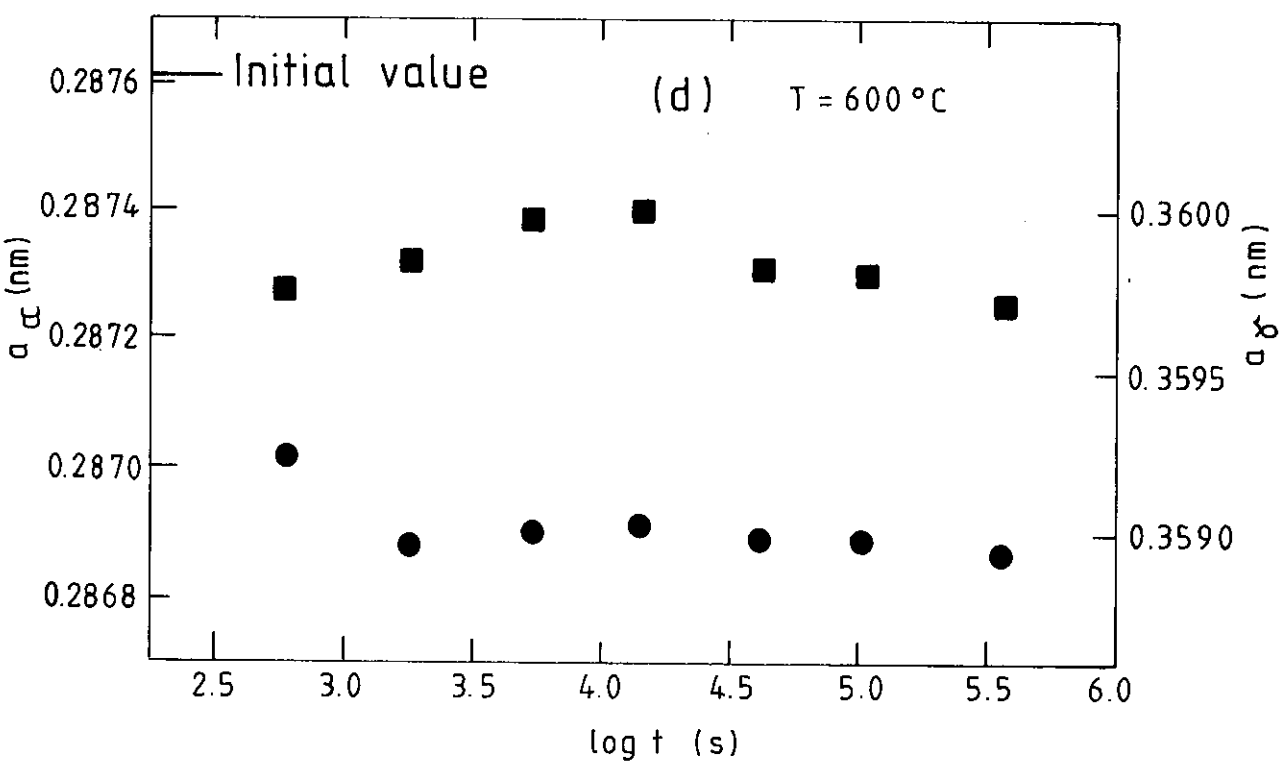

FIGURE 14 (Continued)

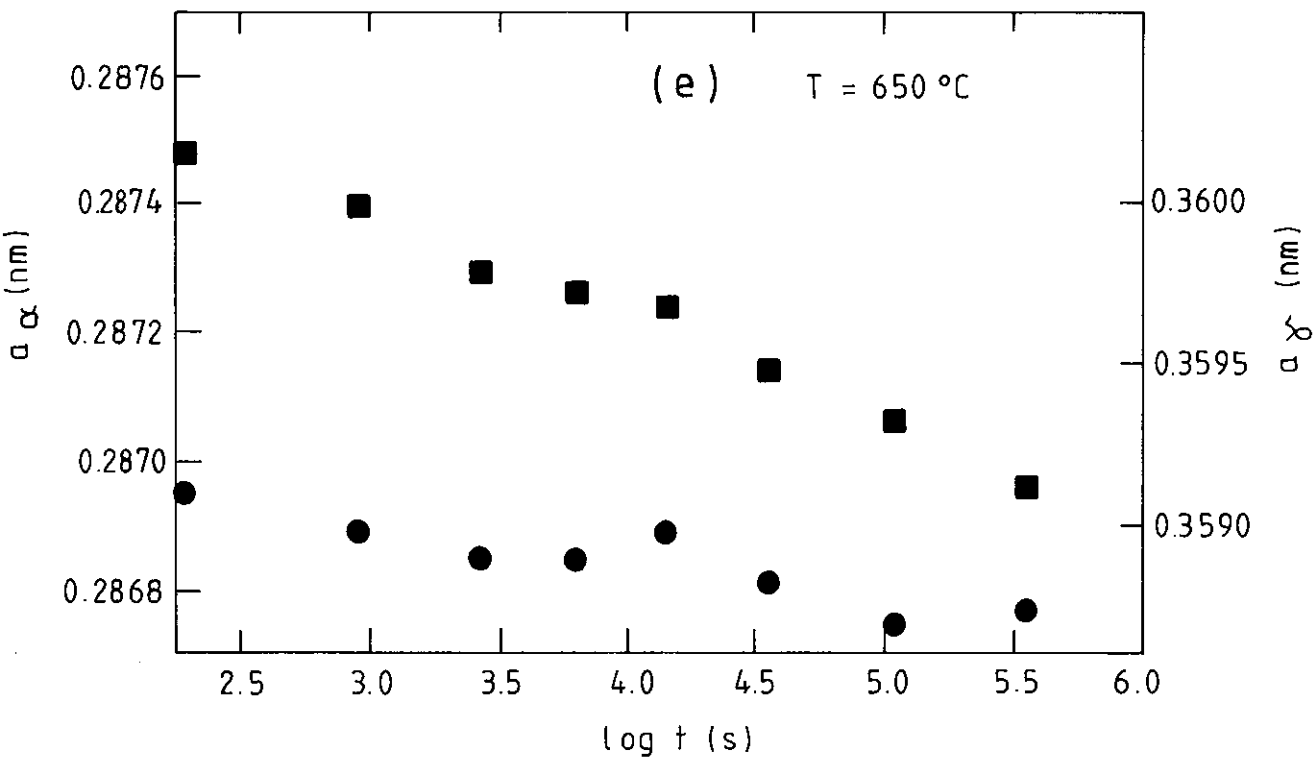

FIGURE 14 (Continued)

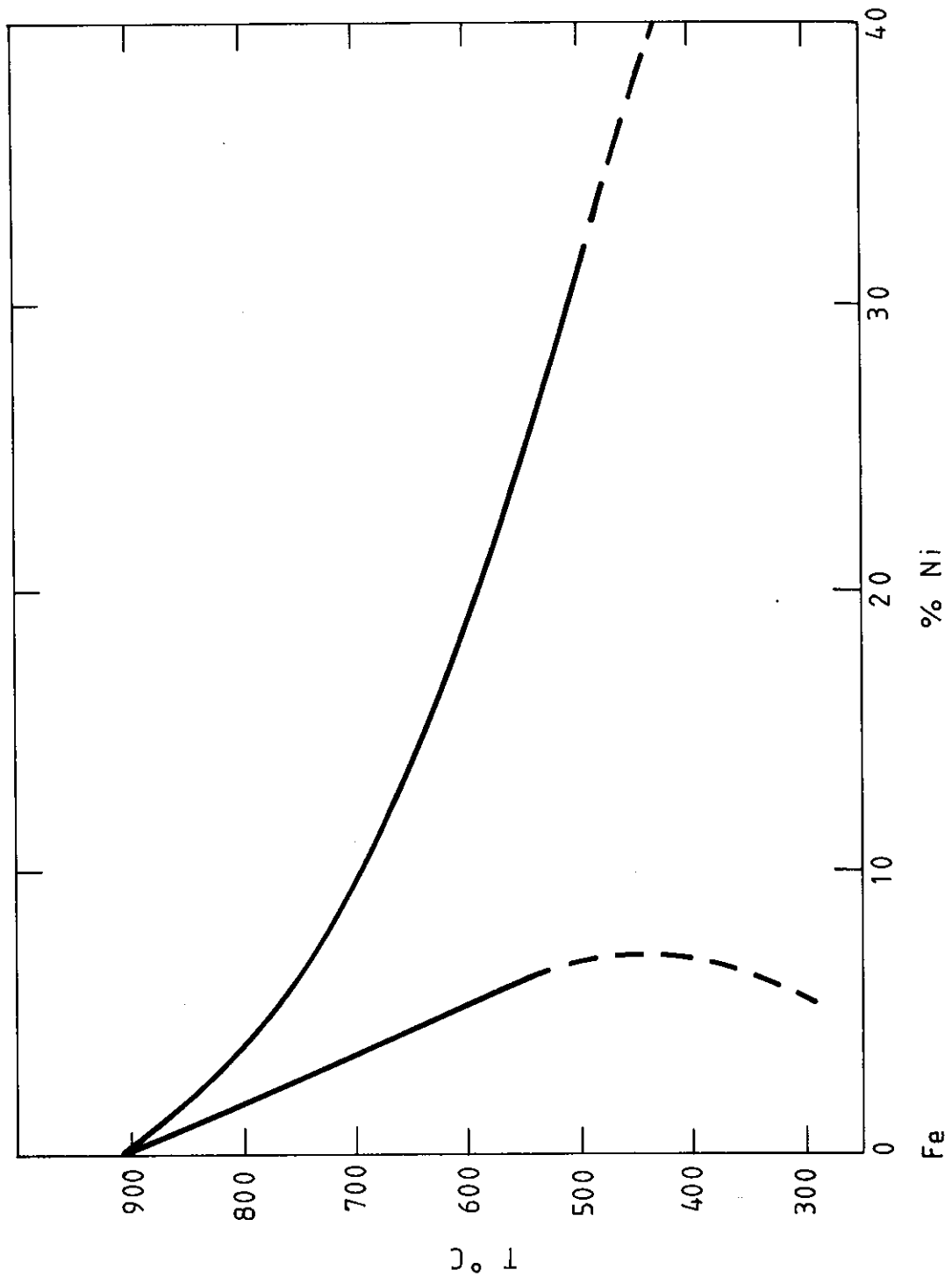

FIGURE 15 Equilibrium diagram of the Fe-Ni binary system [after Goldstein and Ogilvie 1965].

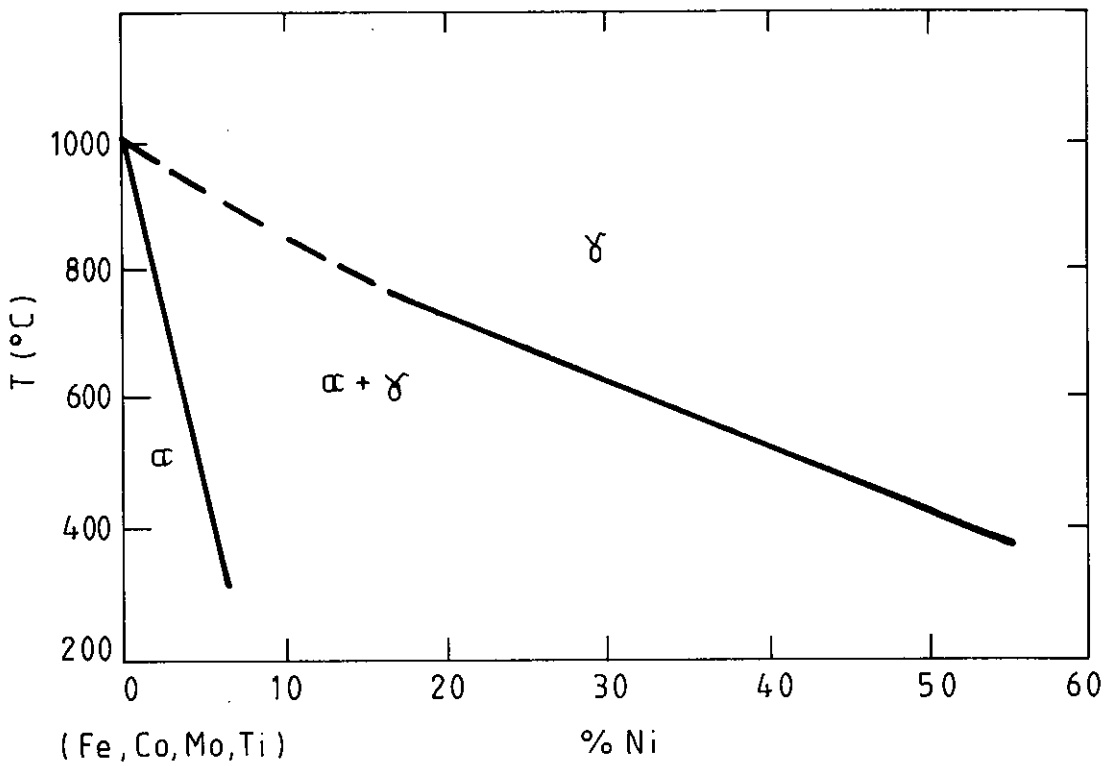

FIGURE 16 Hypothetical equilibrium diagram of the (Fe,9Co,Mo,Ti)-Ni pseudo-binary system.

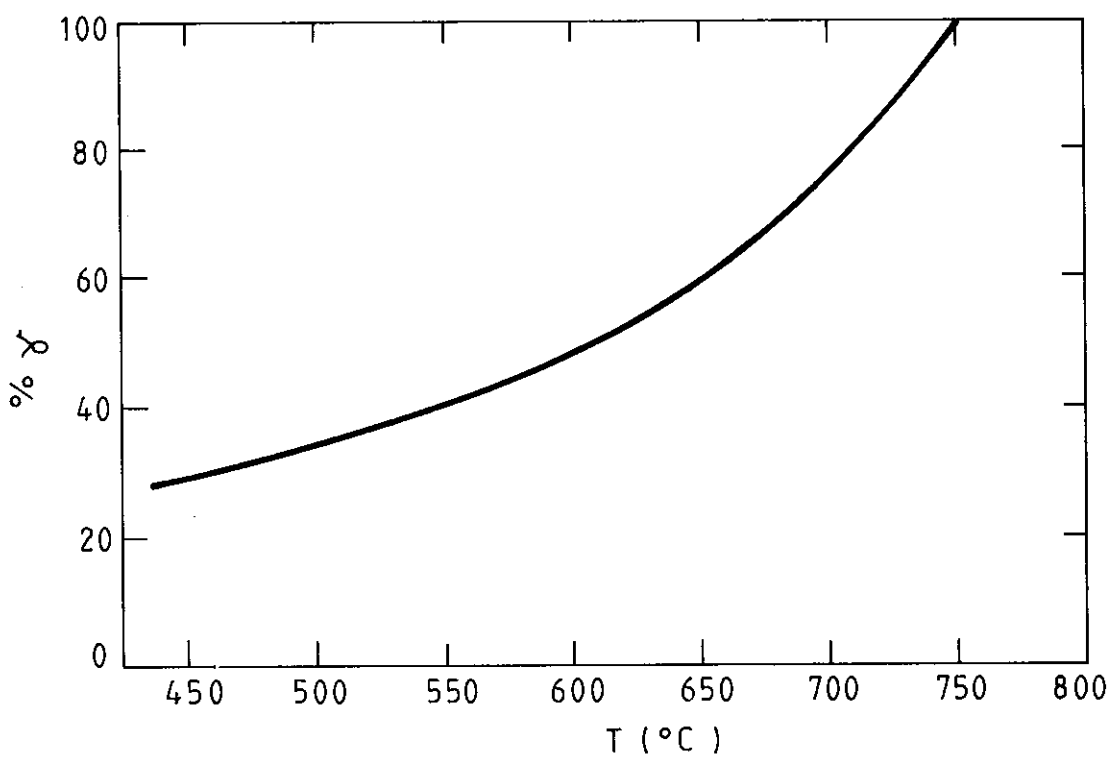

FIGURE 17 Equilibrium amounts of austenite at various temperatures, based on the hypothetical pseudo-binary equilibrium diagram of Figure 16.